Molecular architecture and connectivity of the budding yeast Mtw1 kinetochore complex

Peter Hornung[1], **Michael Maier**[1], **Gregory M Alushin**[2], **Gabriel C Lander**[3], **Eva Nogales**[3,4,5], and **Stefan Westermann**[1,*]

[1] Research Institute of Molecular Pathology, Dr. Bohr Gasse 7, 1030 Vienna, Austria

[2] Biophysics Graduate Group, University of California, Berkeley, Berkeley CA 94720. Department of Molecular and Cell Biology, University of California, Berkeley, Berkeley, CA 94720 USA

[3] Life Science Division, Lawrence Berkeley National Lab, 1 Cyclotron Road, Berkeley, 94720, USA

[4] Life Science Division, Lawrence Berkeley National Lab, 1 Cyclotron Road, Berkeley, CA 94720, USA

[5] Howard Hughes Medical Institute, Chevy Chase, MD, USA

Abstract

Kinetochores are large multi-protein complexes that connect centromeres to spindle microtubules in all eukaryotes. Among the biochemically distinct kinetochore complexes, the conserved four-protein Mtw1 complex is a central part of the kinetochore in all organisms. Here we present the biochemical reconstitution and characterization of the budding yeast Mtw1 complex. Direct visualization by EM revealed an elongated, bi-lobed structure with a 25 nm long axis. The complex can be assembled from two stable heterodimers consisting of Mtw1p-Nnf1p and Dsn1p-Nsl1p and it interacts directly with the microtubule-binding Ndc80 kinetochore complex via the centromere-proximal Spc24/25 head domain. In addition we have reconstituted a partial Ctf19 complex and show that it directly associates with the Mtw1 complex in vitro. Ndc80 and Ctf19 complexes do not compete for binding to the Mtw1 complex, suggesting that Mtw1 can bridge the microtubule-binding components of the kinetochore to the inner centromere.

Keywords

Kinetochore; KMN network; chromosome segregation; force generation; microtubule; centromere

Introduction

The interaction between chromosomes and spindle microtubules requires the action of a complex multi-protein machine termed the kinetochore[1, 2]. Kinetochores are responsible for microtubule-based force generation that drives sister chromatid separation in anaphase. They additionally contain an error-correction mechanism that ensures the bipolar attachments of sister chromatids to opposite spindle poles [3] and they relay signals to the mitotic checkpoint

---

*to whom correspondence should be addressed: Tel. +43 (1) 79730-3450; westermann@imp.ac.at.

that prevents the cell from entering anaphase in the presence of unattached kinetochores 4. In budding yeast, the structural core of the kinetochore consists of at least seven biochemically distinct subcomplexes that are present in fixed copy numbers in mature budding yeast kinetochores 5 and assemble on centromeric DNA in a hierarchical manner 6. A current challenge in the field is to elucidate the architecture of the kinetochore by defining the binding interfaces between kinetochore complexes. Previous biochemical studies have focused on the reconstitution and functional analysis of two important parts of the budding yeast outer kinetochore: the Dam1 complex and the Ndc80 complex. Both of these complexes directly interact with microtubules and are required for force generation at yeast kinetochores 7; 8. The Dam1 complex has the ability to oligomerize into rings *in vitro* 9; 10, opening up the possibility that a Dam1 ring is a physiologically relevant coupling device for kinetochores on microtubule plus-ends in yeast. Recent experiments have demonstrated that Dam1 is a specialized plus-end tracking complex required for a persistent attachment of the Ndc80 complex to dynamic microtubule ends *in vitro* 11; 12.

The four-protein 180kDa Ndc80 complex is a conserved component of all kinetochores. Biochemical isolations from extracts and *in vitro* reconstitution experiments using *C. elegans* Ndc80 subunits have demonstrated that the complex functions together with the conserved four-protein complex Mtw1 (also called Mis12 or MIND) and the protein KNL-1/ Blinkin (Spc105p in budding yeast) as part of a larger network termed KMN (KNL-1 Mis12 Ndc80) 13. Analysis of temperature-sensitive mutants of MTW1 complex subunits in fission yeast and budding yeast, as well as depletion experiments in worms and human cells, have demonstrated that the complex is essential for kinetochore bi-orientation and chromosome segregation 14; 15; 16. Since biochemical reconstitution experiments have so far only been performed with *C. elegans* kinetochore proteins, it is an open question whether the architecture, topology and biochemical activities of the KMN network are conserved among evolutionary distinct eukaryotes. Furthermore, it is unknown how the KMN network is anchored to the inner kinetochore, a critical step in creating a microtubule attachment site specifically at the centromere. Here, we report the reconstitution and biochemical characterization of the budding yeast Mtw1 complex. Our analysis defines the architecture of this central kinetochore complex and is an important step towards a reconstitution of the full yeast kinetochore.

Results and Discussion

Reconstitution of the four-protein Mtw1 complex

To reconstitute the budding yeast Mtw1 complex, we employed a poly-cistronic expression strategy. Genes encoding all four subunits (DSN1, MTW1, NNF1 and NSL1) of the complex were placed under the control of a T7 promoter and expressed in BL21 DE3 cells. The purification strategy used a 6xhistidine tag on the Nnf1p subunit allowing initial purification with a Ni-NTA resin. After elution, the complex was further purified by size exclusion chromatography (Figure 1A). Analysis of the complex on Coomassie stained gels revealed that all four subunits of the complex were present in 1:1:1:1 stoichiometry. The complex eluted earlier than expected from a size exclusion chromatography with a Stokes radius of 74.3 Å. The sedimentation coefficient of the Mtw1 complex was determined by glycerol gradient centrifugation and estimated to be 6S (data not shown). Thus, the native molecular weight of the recombinant complex is 183 kDa, compared to the calculated molecular weight of 148 kDa, and the frictional coefficient f/f_0 is 2.0, predicting a complex that is moderately to highly elongated. These values are in close agreement to those obtained for the Mtw1 complex in yeast extracts 17 suggesting that the recombinant complex closely resembles its native counterpart. We noticed that the Dsn1p subunit of the complex was particularly prone to proteolytic degradation during purification (Figure 1A). Sequencing of the major proteolysis products revealed that the N-terminus of Dsn1p is easily cleaved. We

subsequently cloned an N-terminally shortened version of the Dsn1 subunit corresponding to the major proteolysis product, which lacks amino acids 1–171. Expression of Dsn1$^{172-567}$ in combination with full-length MTW1, NNF1-6xHIS and NSL1 allowed the purification of the entire four-protein Mtw1 complex (Figure 1B). We conclude that the N-terminal extension of Dsn1, which is unusually long in budding yeast compared to other eukaryotes and predicted to be unstructured, is dispensable for complex formation *in vitro*. To determine whether this N-terminal extension has an essential function *in vivo*, we expressed wild-type or N-terminally truncated DSN1$^{172-576}$ on centromeric plasmids in a haploid DSN1 deletion strain that was kept viable by containing a wild-type copy of DSN1 on a CEN-based URA plasmid. Selection against the URA plasmid on 5-FOA plates demonstrated that Dsn1$^{172-576}$ supported wild-type growth (Supplementary Figure 1). Thus, the N-terminal 172 amino acids of Dsn1 are not required for complex formation *in vitro* and do not have an essential function *in vivo*.

The Mtw1 complex can be assembled from two stable heterodimers

SEC analysis of epitope-tagged kinetochore proteins in yeast extracts has suggests that Dam1 and Ndc80 complexes are present only in their fully assembled state, although Mtw1 complexes of different compositions can be detected 17. To identify such stable subcomplexes we expressed various combinations of Mtw1 complex subunits. We were able to express and purify two stable complexes: A heterodimer consisting of Mtw1p and Nnf1p (MN complex) (Figure 1D), and a heterodimer consisting of Dsn1p and Nsl1p (DN complex) (Figure 1C). We next asked whether the Mtw1 heterotetramer can be reconstituted by combining the two stable dimers. After mixing of MN and DN subcomplexes followed by size exclusion chromatography, we observed reconstitution of the full Mtw1 complex, which eluted at a position identical to the native complex (Figure 1E). Thus, the four-protein Mtw1 complex is composed of two stable heterodimers consisting of Mtw1p-Nnf1p and Dsn1p-Nsl1p, a result that is in agreement with binary two-hybrid interactions between these subunits 18.

EM analysis of the reconstituted Mtw1 complex

Negative stain single-particle electron microscopy was used to characterize the structural architecture of the Mtw1 complex. Despite our efforts to cross-link and purify the complex, the imaged fields of particles contained a heterogeneous mixture of aggregates and small fragments, as well as the monomeric, full size complex (Figure 2A). We manually picked the particle images that appeared to correspond to the monomeric, full-length complex based on their consistent size (indicated by white circles in Fig. 2A). After reference-free classification, we observed a distinct bi-lobed rod-like structure approximately 250Å in length, with one of the lobes consistently appearing slightly larger than the other (Figure 2B and D). The larger lobe varied in size, likely reflecting the presence of degrons of the Dsn1p subunit and/or different views around the long axis of the complex.

The larger globular lobe has an approximate diameter of 71 Å, and the smaller lobe 47 Å. Assuming a spherical shape for each, this would correspond to an approximate mass of 150 kDa and 45 kDa, respectively, the sum of which (195 kDa) very closely matches the experimentally determined mass. The calculated mass of the smaller lobe matches well with the combined predicted masses of Mtw1p and Nnf1p (57kDa) assuming that their coiled-coil domains project outwards from the lobe. The calculated mass of the larger lobe exceeds the combined masses of Dsn1p and Nsl1p (91kDa), suggesting that this lobe deviates from spherical geometry (the smaller lobe is too small to accommodate the mass of this subcomplex). The thin density connecting the two globular lobes is approximately 90Å long (Figure 2B), which matches the length of a predicted dimeric coiled-coil between the Mtw1p and Nnf1p subunits (Figure 2C). We also experimentally demonstrated that these two

proteins form a stable subcomplex, supporting the proposal that the coiled-coil regions of these two proteins probably dimerize in the context of the full complex. While this is the most parsimonious explanation for complex topology, we can't exclude the possibility that each globular head is occupied by more than two subunits.

In vivo the Mtw1 complex acts as a bridge between the microtubule-binding Ndc80 complex and the inner kinetochore 6. The Ndc80 complex is 57 nm in length 19, and the Mtw1 complex 25nm. Taken together, these dimensions suggest that the KMN network is long enough to span the full length of the outer kinetochore, consistent with high-resolution fluorescence microscopy studies 20.

Reconstitution of the interaction between Ndc80 and Mtw1 complexes

We next asked whether the recombinant Mtw1 complex can directly interact with the Ndc80 complex. To this end we purified the four-protein Ndc80 complex by expressing the Nuf2-Ndc80 and Spc24-Spc25 heterodimers individually and then reconstituted the entire complex using SEC (Figure 3A). When Mtw1 and Ndc80 complexes were mixed and subjected to gelfiltration, the elution profile of the assembly was shifted with respect to the individual complexes. Coomassie stained gels revealed that the complexes co-eluted, and densitometry of the Coomassie-stained bands indicated a 1:1 stoichiometry of the Mtw1-Ndc80 binary complex (Figure 3B and C). The elution position indicated that the Ndc80-Mtw1 assembly is a dimer containing one copy of each complex. The Ndc80-Mtw1 stoichiometry obtained from this biochemical experiment is in agreement with quantitative fluorescence microscopy data indicating the presence of nearly identical numbers of Ndc80 (8 copies) and Mtw1 (6–7 copies) complexes per each budding yeast kinetochore 5. Another important implication is that budding yeast Ndc80 and Mtw1 complexes form a stable association that does not depend on the presence of the KNL-1 protein Spc105p. This is in contrast to the *in vitro* reconstituted *C. elegans* KMN network, where only a Mis12-Knl1 association is competent to interact with the Ndc80 complex 13. Thus, while the overall association of Ndc80 and Mtw1 complexes is critical for the function of all kinetochores, the molecular details of this association can vary significantly in different organisms. Despite extensive efforts we were unable to express sufficient amounts of full-length or partial Spc105p/KNL-1 fragments, leaving open the possibility that the affinity of the Mtw1 complex for the Ndc80 complex may be increased by the presence of Spc105p.

The two globular domains of the Ndc80 complex have different functions: The Ndc80-Nuf2 head displays microtubule-binding activity through the presence of two Calponin-Homology (CH) domains and a basic N-terminal tail 8; 21. The Spc24/25 head, on the other hand, is thought to reside centromere-proximal and connect the Ndc80 complex to the rest of the kinetochore. We tested which of the Ndc80 subcomplexes provides the binding site for the Mtw1 complex. Therefore we subjected the purified Spc24/25 head of the Ndc80 complex and the Mtw1 complex to size exclusion chromatography first individually and then in combination. Upon pre-incubation with Mtw1 complex, part of the isolated Spc24/25 head was found co-eluting with the Mtw1 complex (Figure 3D and E). The interaction with the head domain seemed to be less efficient when compared to the full Ndc80 complex, suggesting that high-affinity may require the full Ndc80 complex. We conclude that the Ndc80 complex directly binds to the Mtw1 complex via its centromere-proximal Spc24/25 head domain, a result that is in agreement with high resolution microscopy data that place Spc24/25 in the immediate vicinity of Mtw1 complex subunits 20.

Consistent with the results obtained for the *C. elegans* KMN network, the reconstituted Mtw1 complex did not bind directly to taxol-stabilized microtubules in co-sedimentation experiments (Supplementary Figure 2). Only upon inclusion of the purified Ndc80 complex, the Ndc80-Mtw1 assembly was found co-pelleting with microtubules. Furthermore, binding

of the Mtw1 complex did not significantly alter the microtubule-binding properties of the Ndc80 complex (Supplementary Figure 2).

A Ctf19 core complex directly associates with the Mtw1 complex

High-resolution co-localization data place the Mtw1 complex close to the centromere-kinetochore interface 20, but the inner centromere receptor for the complex has not been identified. Human Mis12 complex has been reported to co-purify and directly interact with the inner centromere protein HP1 via the hNSL1 subunit 22; 23. The importance of this interaction for mitotic kinetochore function, however, is unclear and an HP1 homolog is absent from the *Saccharomyces cerevisiae* genome. Biochemical purifications of epitope-tagged Mtw1 subunits from yeast extracts 17; 24 have suggested two candidate interaction partners at the inner centromere interface - the budding yeast CENP-C homolog Mif2p and the Ctf19 complex. Initial experiments failed to detect a direct interaction between recombinant Mif2p fragments and the Mtw1 complex (data not shown), prompting us to focus on the Ctf19 complex as a potential binding partner. The yeast Ctf19 complex is the functional homolog of the constitutive-centromere associated network (CCAN) of higher eukaryotes. The CCAN was originally indentified as a set of polypeptides that co-purify with CENP-A containing nucleosomes 25; 26. The budding yeast Ctf19 complex consists of at least 11 subunits, some of which are organized into more stable subcomplexes. We reconstituted a core Ctf19 complex consisting of the proteins Ctf19p, Okp1p, Mcm21p and Ame1p (also termed COMA 17) by co-expression in *E. coli*. A purification procedure utilizing the 6xHis-tagged Ame1p subunit allowed isolation of the four-protein complex to near homogeneity (Figure 4A). Mcm21, Ame1-6xHis and Ctf19 polypeptides could be resolved on a 20 cm long SDS-PAGE gel (Figure 4A, right panel), and individual bands were excised and analyzed by mass spectrometry. This allowed assignment of the subunits to the corresponding bands on the SDS-PAGE. The intensity of the Coomassie stained bands suggest the presence of all four subunits of the COMA complex in a 1:1:1:1 stoichiometry.

To analyze potential associations with other kinetochore complexes, different concentrations of FLAG-tagged COMA complex were immobilized on beads, incubated with recombinant Mtw1, Ndc80 and Dam1 kinetochore complexes, washed and subsequently eluted with FLAG peptide (Figure 4B). While we failed to detect a direct association of the purified COMA complex with recombinant Ndc80 and Dam1 complexes, the Mtw1 complex consistently co-eluted together with COMA in a concentration-dependent manner (Figure 4C).

To verify the direct interaction between Mtw1 and COMA complexes we performed a reciprocal experiment in which 6xHis-tagged Mtw1, Ndc80 and Dam1 complexes were each immobilized on Ni-NTA agarose, incubated with recombinant Ctf19-Flag core complex, washed and eluted with imidazole. Only in the presence of Mtw1 complex is co-elution of the COMA complex observed (Figure 4C). To more stringently test the physical interaction, we analyzed Mtw1 and COMA complexes by size exclusion chromatography and found that the complexes co-eluted (Figure 5). This result raises the possibility that COMA is involved in recruiting the Mtw1 complex to the inner centromere in budding yeast. A strong prediction from this hypothesis is that Ndc80 and COMA complexes should not compete for binding to the Mtw1 complex. We tested this by pre-incubating Mtw1- and Ndc80 complexes, allowing formation of the binary Mtw1-Ndc80 assembly, followed by incubation with COMA-Flag beads. Incubation with Ndc80 did not prevent the interaction between COMA and Mtw1 complexes and both complexes co-eluted from the beads (Figure 6A). This result indicates that Ndc80 and COMA complexes occupy different binding sites on the Mtw1 complex. When testing the Mtw1-Nnf1 (MN) and Dsn1-Nsl1 (DN) subcomplexes separately in pull-down experiments we found that the MN subcomplex interacted more efficiently with COMA (Figure 6, B and C). Interestingly, of all Mtw1

subunits, high-resolution co-localization data place Nnf1p closest to the inner centromere in both humans and *S. cerevisiae* 27. Since the size of the smaller lobe of the Mtw1 complex roughly fits the combined masses of Mtw1-Nnf1, we tentatively speculate that the larger lobe, predominantly consisting of Dsn1p and Nsl1p, interacts with Spc24/Spc25, while the smaller lobe makes contact to the inner centromere complex COMA. Further antibody decoration experiments and direct visualization by electron microscopy will have to test this hypothesis.

In summary we have characterized the basic architecture of the budding yeast Mtw1 complex. Very recently, two manuscripts have described the reconstitution of the yeast28 and human Mis12 complex29. Our independent results regarding the overall shape of the yeast Mtw1 complex as judged by electron microscopy, its assembly from two stable heterodimers and the high affinity interaction with the Ndc80 complex are in close agreement with the experiments by Maskell et al. A comparison to the human Mis12 complex reveals interesting similarities and differences: The overall architecture of the complex, its topology based on stable Mtw1-Nnf1 and Dsn1-Nsl1 heterodimers is conserved between yeast and human. However, the molecular mechanism by which a high-affinity interaction with the Ndc80 complex is achieved differs considerably between the two organisms. In particular, a yeast Dsn1-Nsl1 heterodimer alone is not competent to bind the Ndc80 complex (our unpublished observations). Yeast Nsl1 lacks a critical binding motif (PVIHL) and a c-terminal tail which is necessary for the interaction between human Nsl1 and the Ndc80 complex 29. Instead, the binding interface between Mtw1 and Ndc80 complexes seems to receive significant contributions from Mtw1 and/or Nnf1. These findings highlight the necessity to analyze kinetochores biochemically in evolutionary distinct organisms in order to reveal common architectural principles and local binding interfaces.

Our results extend the studies by Maskell et al., and Petrovic et al., to provide a potential inner centromere receptor for the Mtw1 complex. The precise molecular basis for the interaction with the yeast Ctf19/COMA complex remains to be investigated. A puzzling aspect is that there is a considerably lower copy number of Ctf19 complex subunits (1–2) versus Mtw1 complexes (6–7) per each budding yeast kinetochore as judged by fluorescence microscopy 5. Furthermore, only OKP1 and AME1 are essential genes in budding yeast 30. It will be important to dissect the molecular binding interface between Ctf19/COMA and Mtw1 complexes in detail and evaluate the disruption of this binding interface *in vivo*. There may be considerable flexibility in the way the KMN network is anchored to the inner centromere. Some organisms like *C. elegans* or *Drosophila melanogaster* for example, seem to lack proteins related to the CCAN network entirely 2. In these kinetochores, the Mtw1 complex may rely on direct interactions with CENP-C for recruitment to the inner centromere.

Materials and Methods

Cloning of polycistronic expression vectors for MTW1 and CTF19

Open reading frames corresponding to Mtw1 complex subunits were amplified from yeast genomic DNA, cloned and expressed using the polycistronic expression system pET3aTr/pST39 that has been described previously 31. Genes were subcloned from the monocistronic pET3aTr vector into the polycistronic cassettes (1–4) of pST39 in the following order for the Mtw1-complex: (1) MTW1, (2) NSL1, (3) NNF1-6xHis, (4) DSN1. The truncated version DSN$^{172–576}$ was cloned into pET28a(+) and expressed in combination with pST39 (MTW1-NSL1-NNF1-6xHis).

The Ctf19 COMA subcomplex was cloned in the following order into the pST39 plasmid: (1) CTF19, (2) MCM21, (3) OKP1 and (4) AME1-6xHis/FLAG. Because of the presence of an intron, MCM21 was amplified from yeast cDNA.

Protein Expression and Purification

The Mtw1 complex was expressed in BL21 DE3 (Novagen) for 4h at 37°C after induction at $OD_{600} = 0.6$ with 0.4 mM isopropyl-β-D-thiogalactopyranosid (IPTG). The coexpression with $DSN^{172-576}$ was performed overnight (o/n) in the presence of 0.2 mM IPTG. The Mtw1 subcomplexes MN and DN were cloned into cassette 1 and 2 of the pST39 vector and the expression conditions were 37°C for 4h (MN) and 18°C overnight (DN). The COMA subcomplex was expressed at 18°C overnight after induction with 0.2 mM IPTG.

Bacteria were lysed by sonication in the presence of protease inhibitors (Roche) and the fusion proteins were isolated using Ni-NTA agarose beads (Qiagen). Binding and subsequent washing was performed in 20 mM HEPES pH 7.0, 300 mM NaCl, 30 mM imidazole. The Mtw1 complex or its two subcomplexes was eluted from Ni-NTA beads with 20 mM Tris pH 8.5, 80 mM NaCl and 250 mM imidazole, subsequently, it was subjected to anion exchange chromatography using a MonoQ 5/50 GL column (GE Healthcare) The column was developed with 10 bed volumes of a linear gradient from 80 mM to 1M NaCl in 20 mM Tris pH 8.5 containing 5% glycerol. The DN-subcomplex was further purified using size exclusion chromatography on a Superose 6 10/30 column.

The COMA-6xHis subcomplex was either purified with Ni-NTA agarose beads or by Anti-FLAG M2 affinity gel (Sigma Aldrich). COMA-6xHis was eluted with 20 mM HEPES pH 7, 150 mM NaCl, 5% Glycerol, 250 mM Imidazol, and loaded onto a size exclusion chromatography (SEC) Superdex 200 HiLoad 16/60 column equilibrated in 20 mM HEPES pH 7, 150 mM NaCl, 5% Glycerol. COMA-FLAG was eluted from M2 affinity gel with 3x FLAG peptide in TBS and the complex was concentrated using ultrafiltration (Vivaspins, cut off 10000 MW) followed by buffer exchange into 20 mM HEPES, pH 7.0, 150 mM NaCl, 5% Glycerol using PD-10 columns (GE Healthcare). Protein concentration was determined with DC Protein Assay kit (Bio-Rad Laboratories).

The Ndc80 and Dam1 kinetochore complexes were expressed and purified as described previously [9; 11; 24].

Interaction studies

0.1 –1 uM kinetochore protein complex in 500 μl binding buffer was immobilized on 20 μl Anti-Flag M2 Affinity gel or 20 μl Ni-NTA agarose beads. The interaction partner to be tested was used at 1 μM in binding buffer (TBS or PBS containing 30 mM imidazole). After incubation for 1h at 4°C, beads were washed three times in either TBS with 0.1% (v/v) NP-40 or in PBS with 30 mM imidazole and complexes were specifically eluted with 3x FLAG peptide or 250 mM imidazole.

Electron Microscopy

Mtw1 complex was thawed and prepared for EM analysis by the GraFix method [32]. 150 μg of the complex was layered on to a 5–40% glycerol gradient in 20mM HEPES pH 7.6, 100mM NaCl, 1mM EDTA, 1mM DTT, which also contained a 0.02 – 0.15% gluteraldehyde gradient, and ultracentrifuged at 55,000 rpm for 13 hours in a TLS55 rotor at 4°C. Fractions were analyzed by SDS-PAGE, and the fraction containing the monomeric cross-linked complex was applied to a glow-discharged C-flat grid (Protochips) augmented with a layer of thin carbon and stained with 2% uranyl formate.

Images were collected on a Gatan 4kx4k CCD camera using a Tecnai F20 electron microscope operating at 120kV and 30,000x magnification. Despite purification by glycerol gradient, the images contained a mixture of aggregates and fragments, as well as the monodispersed full complex. Approximately 5,000 particles that appeared to correspond to the full monomeric complex were picked manually with the BOXER program 33 and subjected to reference-free classification as described 34.

Coiled-coil predictions were performed with the MARCOIL program 35. The regions indicated with grey boxes in Figure 2C correspond to areas of greater than 50% coiled-coil probability, all of which contain regions of greater than 80% coiled-coil probability.

Supplementary Material

Refer to Web version on PubMed Central for supplementary material.

Acknowledgments

Abbreviations

SEC	size exclusion chromatography
MT	microtubule
5-FOA	5-Fluoroorotic Acid

References

1. Cheeseman IM, Desai A. Molecular architecture of the kinetochore-microtubule interface. Nat Rev Mol Cell Biol. 2008; 9:33–46. [PubMed: 18097444]

2. Santaguida S, Musacchio A. The life and miracles of kinetochores. Embo J. 2009; 28:2511–31. [PubMed: 19629042]

3. Tanaka TU, Rachidi N, Janke C, Pereira G, Galova M, Schiebel E, Stark MJ, Nasmyth K. Evidence that the Ipl1-Sli15 (Aurora kinase-INCENP) complex promotes chromosome bi-orientation by altering kinetochore-spindle pole connections. Cell. 2002; 108:317–29. [PubMed: 11853667]

4. Musacchio A, Salmon ED. The spindle-assembly checkpoint in space and time. Nat Rev Mol Cell Biol. 2007; 8:379–93. [PubMed: 17426725]

5. Joglekar AP, Bouck DC, Molk JN, Bloom KS, Salmon ED. Molecular architecture of a kinetochore-microtubule attachment site. Nat Cell Biol. 2006; 8:581–5. [PubMed: 16715078]

6. Westermann S, Drubin DG, Barnes G. Structures and functions of yeast kinetochore complexes. Annu Rev Biochem. 2007; 76:563–91. [PubMed: 17362199]

7. Westermann S, Wang HW, Avila-Sakar A, Drubin DG, Nogales E, Barnes G. The Dam1 kinetochore ring complex moves processively on depolymerizing microtubule ends. Nature. 2006; 440:565–9. [PubMed: 16415853]

8. Ciferri C, Pasqualato S, Screpanti E, Varetti G, Santaguida S, Dos Reis G, Maiolica A, Polka J, De Luca JG, De Wulf P, Salek M, Rappsilber J, Moores CA, Salmon ED, Musacchio A. Implications for kinetochore-microtubule attachment from the structure of an engineered Ndc80 complex. Cell. 2008; 133:427–39. [PubMed: 18455984]

9. Westermann S, Avila-Sakar A, Wang HW, Niederstrasser H, Wong J, Drubin DG, Nogales E, Barnes G. Formation of a dynamic kinetochore- microtubule interface through assembly of the Dam1 ring complex. Mol Cell. 2005; 17:277–90. [PubMed: 15664196]

10. Miranda JJ, De Wulf P, Sorger PK, Harrison SC. The yeast DASH complex forms closed rings on microtubules. Nat Struct Mol Biol. 2005; 12:138–43. [PubMed: 15640796]

11. Lampert F, Hornung P, Westermann S. The Dam1 complex confers microtubule plus end-tracking activity to the Ndc80 kinetochore complex. J Cell Biol. 189:641–9. [PubMed: 20479465]

12. Tien JF, Umbreit NT, Gestaut DR, Franck AD, Cooper J, Wordeman L, Gonen T, Asbury CL, Davis TN. Cooperation of the Dam1 and Ndc80 kinetochore complexes enhances microtubule coupling and is regulated by aurora B. J Cell Biol. 189:713–23. [PubMed: 20479468]

13. Cheeseman IM, Chappie JS, Wilson-Kubalek EM, Desai A. The conserved KMN network constitutes the core microtubule-binding site of the kinetochore. Cell. 2006; 127:983–97. [PubMed: 17129783]

14. Goshima G, Kiyomitsu T, Yoda K, Yanagida M. Human centromere chromatin protein hMis12, essential for equal segregation, is independent of CENP-A loading pathway. J Cell Biol. 2003; 160:25–39. [PubMed: 12515822]

15. Cheeseman IM, Niessen S, Anderson S, Hyndman F, Yates JR 3rd, Oegema K, Desai A. A conserved protein network controls assembly of the outer kinetochore and its ability to sustain tension. Genes Dev. 2004; 18:2255–68. [PubMed: 15371340]

16. Kline SL, Cheeseman IM, Hori T, Fukagawa T, Desai A. The human Mis12 complex is required for kinetochore assembly and proper chromosome segregation. J Cell Biol. 2006; 173:9–17. [PubMed: 16585270]

17. De Wulf P, McAinsh AD, Sorger PK. Hierarchical assembly of the budding yeast kinetochore from multiple subcomplexes. Genes Dev. 2003; 17:2902–21. [PubMed: 14633972]

18. Kiyomitsu T, Obuse C, Yanagida M. Human Blinkin/AF15q14 is required for chromosome alignment and the mitotic checkpoint through direct interaction with Bub1 and BubR1. Dev Cell. 2007; 13:663–76. [PubMed: 17981135]

19. Wang HW, Long S, Ciferri C, Westermann S, Drubin D, Barnes G, Nogales E. Architecture and flexibility of the yeast Ndc80 kinetochore complex. J Mol Biol. 2008; 383:894–903. [PubMed: 18793650]

20. Joglekar AP, Bloom K, Salmon ED. In vivo protein architecture of the eukaryotic kinetochore with nanometer scale accuracy. Curr Biol. 2009; 19:694–9. [PubMed: 19345105]

21. Wei RR, Al-Bassam J, Harrison SC. The Ndc80/HEC1 complex is a contact point for kinetochore-microtubule attachment. Nat Struct Mol Biol. 2006

22. Obuse C, Iwasaki O, Kiyomitsu T, Goshima G, Toyoda Y, Yanagida M. A conserved Mis12 centromere complex is linked to heterochromatic HP1 and outer kinetochore protein Zwint-1. Nat Cell Biol. 2004; 6:1135–41. [PubMed: 15502821]

23. Kiyomitsu T, Iwasaki O, Obuse C, Yanagida M. Inner centromere formation requires hMis14, a trident kinetochore protein that specifically recruits HP1 to human chromosomes. J Cell Biol. 188:791–807. [PubMed: 20231385]

24. Westermann S, Cheeseman IM, Anderson S, Yates JR 3rd, Drubin DG, Barnes G. Architecture of the budding yeast kinetochore reveals a conserved molecular core. J Cell Biol. 2003; 163:215–22. [PubMed: 14581449]

25. Foltz DR, Jansen LE, Black BE, Bailey AO, Yates JR 3rd, Cleveland DW. The human CENP-A centromeric nucleosome-associated complex. Nat Cell Biol. 2006; 8:458–69. [PubMed: 16622419]

26. Okada M, Cheeseman IM, Hori T, Okawa K, McLeod IX, Yates JR 3rd, Desai A, Fukagawa T. The CENP-H-I complex is required for the efficient incorporation of newly synthesized CENP-A into centromeres. Nat Cell Biol. 2006; 8:446–57. [PubMed: 16622420]

27. Wan X, O'Quinn RP, Pierce HL, Joglekar AP, Gall WE, DeLuca JG, Carroll CW, Liu ST, Yen TJ, McEwen BF, Stukenberg PT, Desai A, Salmon ED. Protein architecture of the human kinetochore microtubule attachment site. Cell. 2009; 137:672–84. [PubMed: 19450515]

28. Maskell DP, Hu XW, Singleton MR. Molecular architecture and assembly of the yeast kinetochore MIND complex. J Cell Biol. 190:823–34. [PubMed: 20819936]

29. Petrovic A, Pasqualato S, Dube P, Krenn V, Santaguida S, Cittaro D, Monzani S, Massimiliano L, Keller J, Tarricone A, Maiolica A, Stark H, Musacchio A. The MIS12 complex is a protein interaction hub for outer kinetochore assembly. J Cell Biol. 190:835–52. [PubMed: 20819937]

30. Ortiz J, Stemmann O, Rank S, Lechner J. A putative protein complex consisting of Ctf19, Mcm21, and Okp1 represents a missing link in the budding yeast kinetochore. Genes Dev. 1999; 13:1140–55. [PubMed: 10323865]

31. Tan S. A modular polycistronic expression system for overexpressing protein complexes in Escherichia coli. Protein Expr Purif. 2001; 21:224–34. [PubMed: 11162410]

32. Kastner B, Fischer N, Golas MM, Sander B, Dube P, Boehringer D, Hartmuth K, Deckert J, Hauer F, Wolf E, Uchtenhagen H, Urlaub H, Herzog F, Peters JM, Poerschke D, Luhrmann R, Stark H. GraFix: sample preparation for single-particle electron cryomicroscopy. Nat Methods. 2008; 5:53–5. [PubMed: 18157137]

33. Ludtke SJ, Baldwin PR, Chiu W. EMAN: semiautomated software for high-resolution single-particle reconstructions. J Struct Biol. 1999; 128:82–97. [PubMed: 10600563]

34. Ramey VH, Wang HW, Nogales E. Ab initio reconstruction of helical samples with heterogeneity, disorder and coexisting symmetries. J Struct Biol. 2009; 167:97–105. [PubMed: 19447181]

35. Delorenzi M, Speed T. An HMM model for coiled-coil domains and a comparison with PSSM-based predictions. Bioinformatics. 2002; 18:617–25. [PubMed: 12016059]
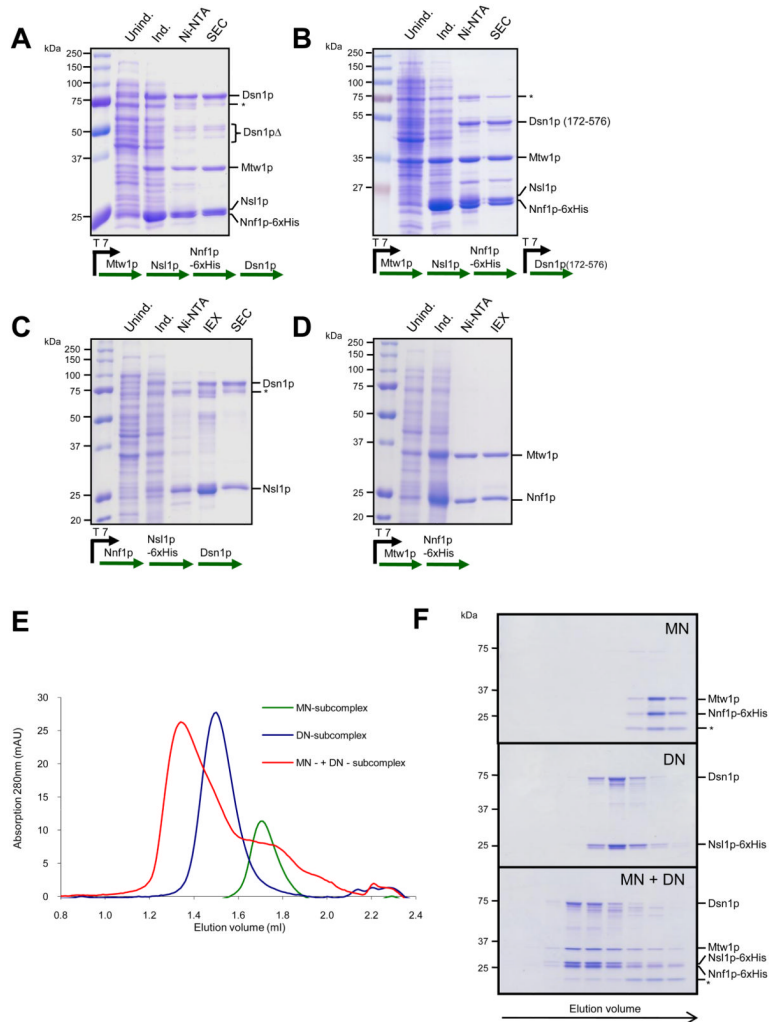
Figure 1. Reconstitution of the Mtw1 complex
A. Expression and purification of the Mtw1 complex. The coomassie-stained gel shows different steps of the purification scheme: control extract and extract after induction with IPTG, eluate from Ni-NTA beads and purified fraction after SEC. Note the presence of degradation products of the Dsn1p subunit. **B**. Expression and purification of a complex with an N-terminally truncated Dsn1p subunit. **C**. Expression and purification of a stable Dsn1-Nsl1 heterodimer. IEX denotes anion exchange chromatorgraphy. Asterisks in A, B and C indicate a contamination with the *E. coli* Hsp70 chaperone **D**. Expression and purification of Mtw1-Nnf1 heterodimer. **E**. SEC runs of Dsn1p-Nsl1p and Mtw1p-Nnf1p subcomplexes (8 μM each) and of the full complex after reconstitution. **F**. Coomassie-stained SDS-PAGE of fractions from E. Asterisks indicate an Nnf1 truncation product.
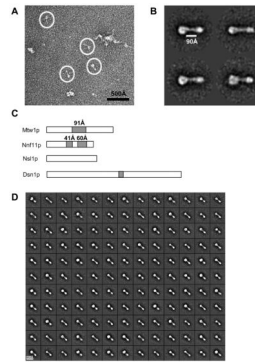
Figure 2. EM analysis of the Mtw1 complex
A. Negative stain EM image of the Mtw1 complex. Note the heterogeneous composition of the sample. White circles correspond to particles chosen for further analysis. **B**. Selected class averages showing the architecture and dimensions of the complex. The complex is a bi-lobed rod, with one large and one small globular domain. **C**. Coiled-coil predictions for the protein subunits of the complex. Grey regions correspond to greater than 50% coiled-coil probability. **D**. Entire complement of class averages obtained for the complex. They all display the bi-lobed architecture, with most heterogeneity occurring in the size of the larger globular domain.
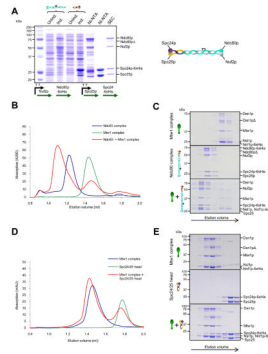
Figure 3. The Mtw1 complex interacts with Ndc80 via the Spc24/25 head
A. Expression and purification of the Ndc80 kinetochore complex. The Ndc80-Nuf2 and Spc24-Spc25 heterodimers are expressed individually and after combination the reconstituted full complex is purified by SEC. **B**. Coomassie-stained gels of gelfiltration runs of Mtw1 complex and Ndc80 complex alone, or after combination (9 μM each). **C**. Gelfiltration profile corresponding to B. **D**. Coomassie-stained gels of Mtw1 complex and purified Spc24/25 head domain alone, or after combination (6 μM each). **E**. Gelfiltration profile corresponding to D.
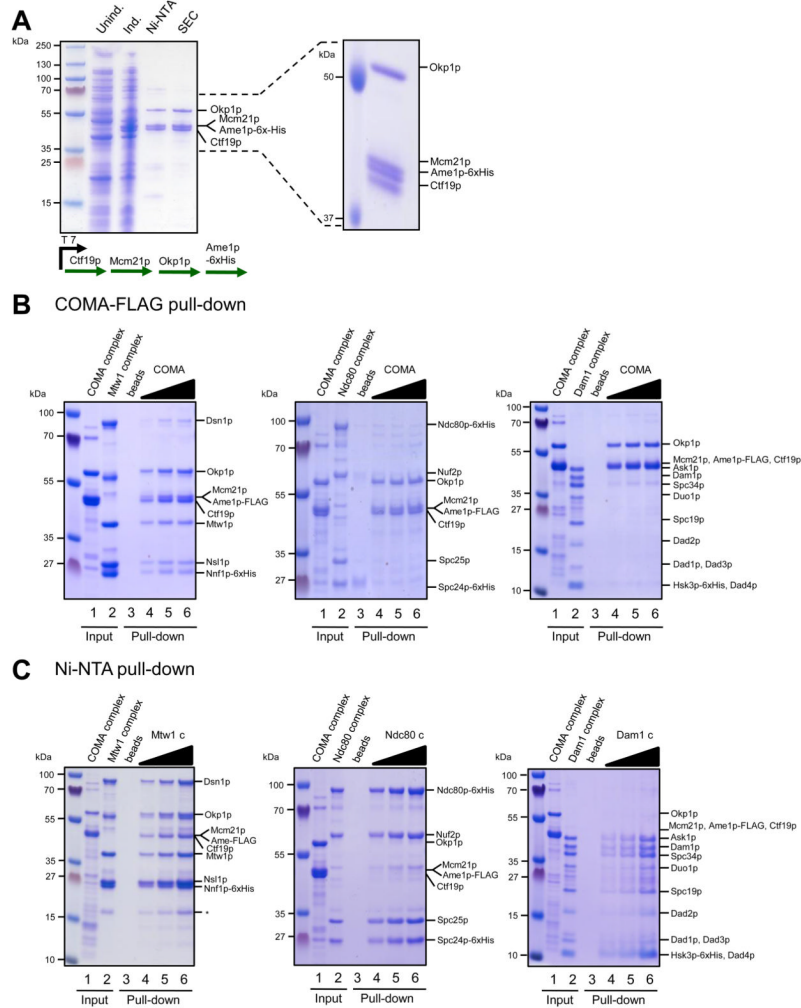
Figure 4. Reconstitution of a Ctf19 core complex (COMA) and interaction with Mtw1
A. Reconstitution of the Ctf19-Okp1-Mcm21-Ame1 complex (COMA). Coomassie stained gel of different stages of the purification. Right panel: The four polypeptides of the complex are resolved on large SDS-PAGE gels. **B.** Pull-down experiment with immobilized COMA complex. Different amounts of recombinant COMA complex (lane 1) were immobilized on Anti-FLAG M2 affinity gel and incubated with Mtw1, Ndc80 or Dam1 complex (lane 2). Control pull-downs contained only M2 beads (lane 3). After washing, bound complexes were eluted with FLAG-peptide (lane 4–6). Note that the Mtw1 complex co-elutes with COMA from the beads. **C**. COMA-Flag complex (lane 1) was incubated with His-tagged Mtw1-, Ndc80 or Dam1 complex which were immobilized on Ni-NTA beads (lane 2, lane 3 denotes Ni-NTA beads as a negative control). After washing, bound complexes were eluted with imidazole (lanes 4–6). Note that the COMA complex is co-eluted with the Mtw1 complex from Ni-NTA beads.
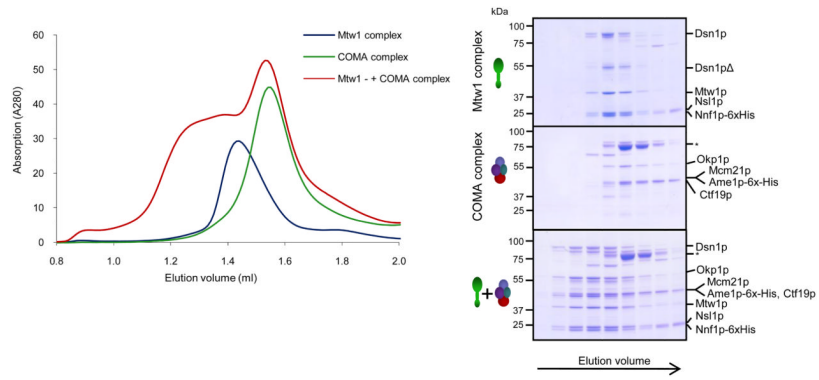
Figure 5. Size-exclusion chromatography of Mtw1 and COMA complexes
Coomassie-stained gels and gelfiltration profiles of Mtw1 complex and Ndc80 complex
individually, or after combination (5 µM each). Asterisk indicates Hsp70 contamination in
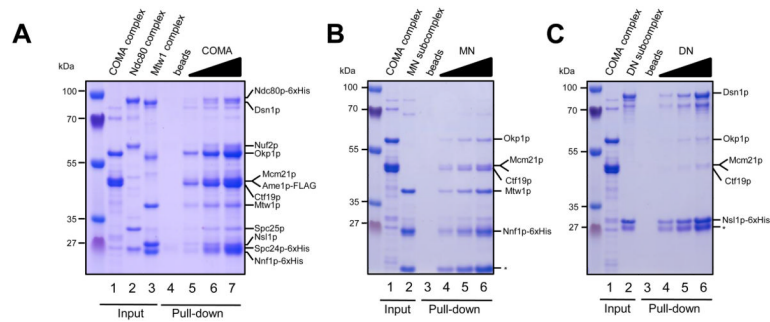the COMA complex sample.

Figure 6. Ndc80 and the COMA complex bind non-competitively to the Mtw1 complex
A. COMA-flag complex (lane1) was immobilized on M2 beads. Mtw1 (lane2) and Ndc80 complexes (lane 3) were pre-mixed and incubated with control-beads (lane 4) or COMA-flag beads. After washing, bound complexes were eluted with Flag peptide (lanes 5–7). **B.** Pull-down experiment using 6xHis tagged MN-subcomplex on Ni-NTA agarose and and FLAG-tagged COMA complex. Note co-elution of the complexes from the Ni-NTA beads. Asterisk indicates Nnf1 truncation product **C**. Pull-down experiment using 6xHis tagged DN-subcomplex on Ni-NTA agarose and FLAG-tagged COMA complex. The COMA complex fails to interact with the DN subcomplex. Asterisk denotes Nsl1 truncation product.